Supporting information

Kinetics and mechanism for thermal and photochemical decomposition of 4,4'-azobis(4-cyanopentanoic acid) in aqueous media

Yanyan Zhou,[a,b] Zhengbiao Zhang,[a*] Almar Postma[b] and Graeme Moad[b*]

Materials. 4,4′-azobis(4-cyanopentanoic acid) (ACPA, Sigma-Aldrich, 98%) was recrystallized from methanol before use, sodium carbonate and 3-(trimethylsilyl) propionic-2,2,3,3-d_4 acid sodium salt (TMSP-d_4) were obtained from Sigma-Aldrich and used as received. All solvents were used as received.

Instrumentation. Nuclear magnetic resonance (NMR) spectra were obtained using a Bruker AV-400 (400 MHz) or a AV-500 (500 MHz) spectrometer using D_2O or DMF-d_7 as NMR solvent.

Mass spectrometric (MS) analyses were performed on a Waters Acquity UPLC i-Class with QDa performance mass detector with an adjustment-free atmospheric pressure ionisation (API) electrospray (ES) interface. Positive and negative ions were recorded simultaneously with full scan analysis in the range m/z 50 to 1000. High purity nitrogen (>95%) nebulizing/desolvation gas was used for vaporization with the pressure regulated at 650-700 kPa. The Probe temperature was set at 600 °C, the source temperature at 120 °C, the cone voltage was 10 V whilst the capillary voltage was 0.8 kV for both positive and negative ion spectra.

An Acquity UPLC BEH C_{18} Column (50 × 2.1 mm, 1.7 µm particle size) was used. Mobile Phase A was 100% Milli-Q Water with 0.1% formic acid. Mobile Phase B was 100% Acetonitrile with 0.1% formic acid. The eluting conditions involved a gradient (95% A to 100% B over 4.50 minutes) and maintaining at 100% B for >1 minute. The flow rate was 0.400 mL min^{-1} and the column temperature was 30 °C. The MS collected data for the entire run. The diode array spectral analysis covered the wavelength range 190 to 350 nm with the chromatogram shown being extracted for 195 nm. The sample injection volume was 1 µL.

Procedures.

Photo-decomposition of ACPA in D_2O. A solution of ACPA (28 mg, 0.1 mmol) and TMSP-d_4 (2.5 mg, NMR internal standard) was prepared in D_2O (2 mL) containing sodium carbonate (21.2 mg, 0.2 mmol) to form a clear solution. An aliquot (0.6 mL) of this solution was transferred to a sealable NMR tube. The solution was degassed by three freeze-pump-thaw cycles, backfilled with nitrogen, and flame sealed. The NMR tube was placed in a jacketed holder in a photo-reactor with violet light (402 nm, 17 W) irradiation. The temperature was controlled at ~25 °C with water that was circulated

through the jacket from a thermostatted bath maintained at 25 °C by means of a peristaltic pump. The NMR tube was removed from the reactor and NMR-data collected at two-hourly intervals. The NMR tube was protected from ambient light between irradiation periods.

The photoreactor used for these experiment has been described elsewhere.[1] The visible light reactor was constructed using ACULED VHL™ (Very High Lumen) LEDs procured from Excelitas Technologies with emission λ_{max} measured at 402 nm (violet light). The LEDs were housed in a rectangular aluminium box with 9 LEDs on each wall of the housing. Intensity measurements using a Silverline all UV radiometer (230 – 410 nm) were conducted to estimate the average emission intensity. The calibration curve (Figure S1) indicates that for 17 W (the minimum power setting for the reactor) the emission intensity is approximately zero. However, the small sample cavity meant that the photodiode was held at the top of the reactor and the emission intensities are most likely an underestimate. If it is assumed the line should pass through zero and simply offset then an estimated (maximum) emission intensity is 4 mW/cm^2.

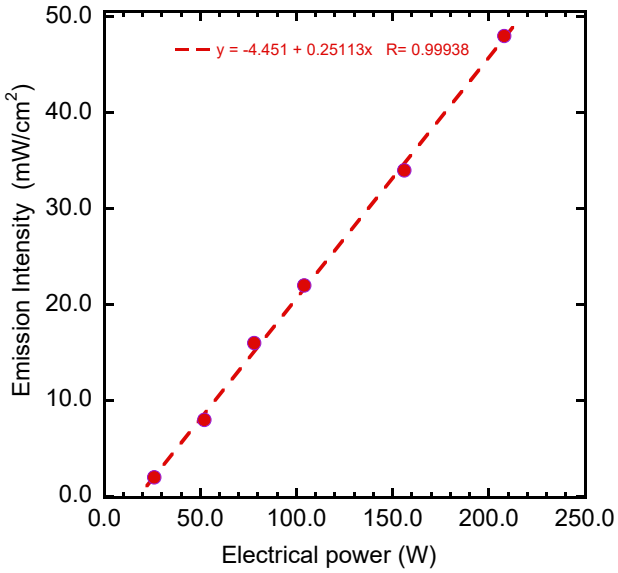

Figure S1. Average emission intensity *vs* electrical power for the 402 nm light source.

Thermal-decomposition of ACPA in D_2O. The sample was prepared followed using the above-mentioned procedure. The sealed NMR tube was placed in a thermostatted oil bath thermostatted at the required temperature. Thermal-decomposition experiments in D_2O were performed at 50.0, 60.0, 70.0 and 80.0±0.1 °C. The NMR tube was removed from the oil bath and cooled rapidly in an ice bath before NMR-data acquisition at two-hourly intervals.

Photo-decomposition of ACPA in DMF-d_7. A solution of ACPA (7 mg, 0.025 mmol) was prepared in DMF-d_7 (0.5 mL) and transferred to a NMR tube. The solution was degassed by three freeze-pump-thaw cycles, backfilled with nitrogen, and flame sealed. The NMR tube was placed in a jacketed holder in a photo-reactor with violet light (402

nm, 17 W) irradiation.[1] The temperature was controlled at ~25 °C with pre-heated water that was circulated through the jacket from a thermostatted bath by means of a peristaltic pump. The NMR tube was removed from the reactor and NMR-data collected at 30 minute intervals. Refer Figure S12 (NMR spectra), Figure S13 (time evolution of products), and Figure S14 (disproportionation products).

Thermal-decomposition of ACPA in DMF-d_7. A solution of initiator ACPA (7 mg, 0.025 mmol) was prepared in DMF-d_7 (0.5 mL) and transferred to a NMR tube. The mixture was degassed by three freeze-pump-thaw cycles, backfilled with nitrogen, and flame sealed. The NMR tube was placed in a thermostatted oil bath preheated to 80.0±0.1 °C. The NMR tube was removed from the oil bath and cooled rapidly in an ice bath before NMR-data acquisition at required intervals as dictated by the reaction temperature. Refer Figure S10 (NMR spectra), Figure S11 (time evolution of products) and Figure S16 (rate constant determination).

NMR spectra in D_2O. Partial ^{13}C NMR and ^{1}H NMR spectra (D_2O) and signal assignments are provided below. Assignments are based on the literature NMR spectra, ^{1}H NMR (CF_3COOD and/or acetone-d_6) spectra for *meso*- and *rac*-**A**, **D** (two diastereomers), **E**, **F**, **G** and **H** are reported by Overberger and Labianca,[2] supported by 2D NMR spectra (which include Figure S4-Figure **S6**). A signal at 1.33 ppm was observed only for thermal decomposition at 50 °C (0.2 M Na_2CO_3) and at 70 °C with a lower concentration of Na_2CO_3 (0.1 M). The signal, which is partially overlapped with signal for **E**, is consistent with the ketenimine **C**, or (more likely) another product derived from the ketenimine **C**, based on kinetics of its appearance and its stable in solution at ambient temperature.

Where an asterisk appears following a chemical shift in the following listing, the NMR signal could not be seen directly due to peak overlap. However, it was possible to ascertain the chemical shift from 2D NMR (HMBC or HSQC) spectra.

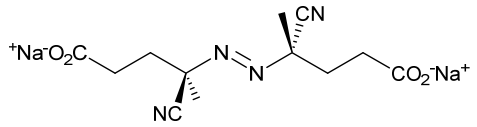

meso-**A**

meso-**A**:[2] ^{1}H NMR (D_2O) δ 1.81 (s, 6H, CH_3), 2.00-2.40 (m, C**H**$_2$), ^{13}C NMR δ 23.18 (**C**H_3), 32.46 (**C**H_2COONa), 34.01 (C**C**H_2), 72.98 (**C**CH_2), 118.9 (**C**N), 180.49 (**C**OONa).

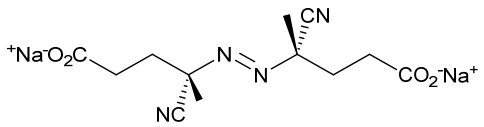

rac-**A**

rac-**A**:[2] ^{1}H NMR (D_2O) δ 1.76 (s, 6H, CH_3), 2.00-2.40 (C**H**$_2$) ^{13}C NMR δ 22.80 (**C**H_3), 32.32 (**C**H_2COONa), 34.07 (C**C**H_2), 72.80 (**C**CH2), 119.26 (**C**N), 180.57 (**C**OONa).

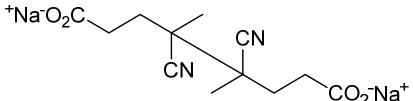

D

2 diastereoisomers

D (LMDA): ^{1}H NMR (D_2O) δ 1.52 (s, 6H, CH_3), ^{13}C NMR δ 30.5 (C**C**H_2), 44.3 (**C**CH_2), 122.1 (**C**N). Tentatively assigned as the low melting diastereoisomer (LMDA) based on relative NMR chemical shift and data reported by Overberger and Labianca.[2]

D (HMDA): ^{1}H NMR (D_2O) δ 1.54 (s, 6H, CH_3), ^{13}C NMR δ 30.5 (C**C**H_2), 44.3 (**C**CH_2), 122.2 (**C**N). Tentatively assigned as the high melting diastereoisomer (HMDA) based on relative NMR chemical shift.[2]

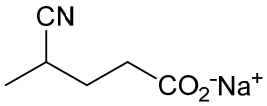

E

E:[2] ^{1}H NMR (D_2O) δ 1.34 (d, *J*=7.12 Hz, 3H, C**H**$_3$CH(CN)), 2.82 (m, 1 H, CH_3C**H**(CN)), 1.88 (m, 2H, CHC**H**$_2$), 2.37* (m, 2H, C**H**$_2$CO), ^{13}C NMR δ 16.9 (**C**H_3CH(CN)), 24.8 (CH_3**C**H(CN)), 29.9 (CH**C**H_2), 31.3 (**C**H_2CO), 124.6 (**C**N), 181.8 (**C**OONa)

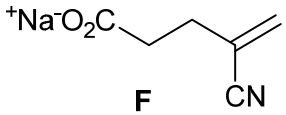

F

F:[2] ^{1}H NMR (D_2O) δ 6.02 (t, *J*=1.1 Hz, 1H, C=C**H**H (*trans* to nitrile)), 5.94 (t, *J*=1.5 Hz, 1H, C=CH**H** (*cis* to nitrile)), 2.56* (2H, C**H**$_2$(CN)C=). ^{13}C NMR δ 30.2 (**C**H_2C), 119.4 (**C**N), 121.2 (**C**=CH_2), 132.5 (C=**C**H_2), 181.0 (**C**OONa).

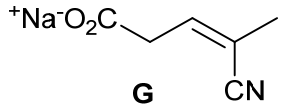

G

G:[2] ^{1}H NMR (D_2O) δ 6.46 (t, *J*=7.75 Hz, 1H, (COONa)CH_2C**H**=), 3.30 (d, *J* = 7.62 Hz, 2H, (COONa)C**H**$_2$CH=), 2.02 (3H, =C(CN)C**H**$_3$), ^{13}C NMR δ 110.46 (=**C**(CN)CH_3), 119.05 (**C**N), 143.74 (**C**H=C(CN)CH_3), 178.17 (**C**OONa). Signals assigned on basis of 2D NMR.

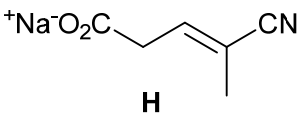

H

H:[2] ^{1}H NMR (D_2O) δ 6.62 (t, *J* = 7.06 Hz, 1H, (COONa)CH_2C**H**=), 3.21(d, *J* = 7.84 Hz, 2H, (COONa)C**H**$_2$CH=), 1.93* (3H, =C(CN)C**H**$_3$), ^{13}C NMR δ 110.08 (=**C**(CN)CH_3), 119.22 (**C**N), 144.07 (**C**H=C(CN)CH_3), 178.17 (**C**OONa). Signals assigned on basis of 2D NMR.

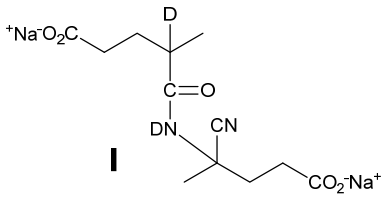

I

2 diastereoisomers

I (diastereoisomer 1): ^{1}H NMR (D_2O) δ 1.13 (s, 3H, CDC**H**$_3$), 1.67 (3H, C(CN)C**H**$_3$), 1.69* (1H, C**H**HCD), 1.82* (1 H, CH**H**CD), ^{13}C NMR δ 16.46 (CD**C**H$_3$), 29.94 (**C**H$_2$CD), 34.98 ((COONa)**C**H$_2$CH$_2$CD), 34.6 (C**C**H$_2$), 39.5 (**C**DCH$_3$), 49.86 (**C**(CN)CH$_3$), 120.60 (CN), 179.40 (**C**OND), 182.50 (**C**OONa).

I (diastereoisomer 2): ^{1}H NMR (D_2O) δ 1.14 (s, 3H, CDC**H**$_3$) 1.68 (3H, C(CN)C**H**$_3$), 1.69* (1H, C**H**HCD), 1.82* (1 H, CH**H**CD), ^{13}C NMR δ 16.46 (CD**C**H$_3$), 29.94 (**C**H$_2$CD), 34.98 ((COONa)**C**H$_2$CH$_2$CD), 34.60 (C**C**H$_2$), 39.50 (**C**DCH$_3$), 49.86 (**C**(CN)CH$_3$), 120.60 (CN), 179.40 (**C**OND), 182.50 (**C**OONa).

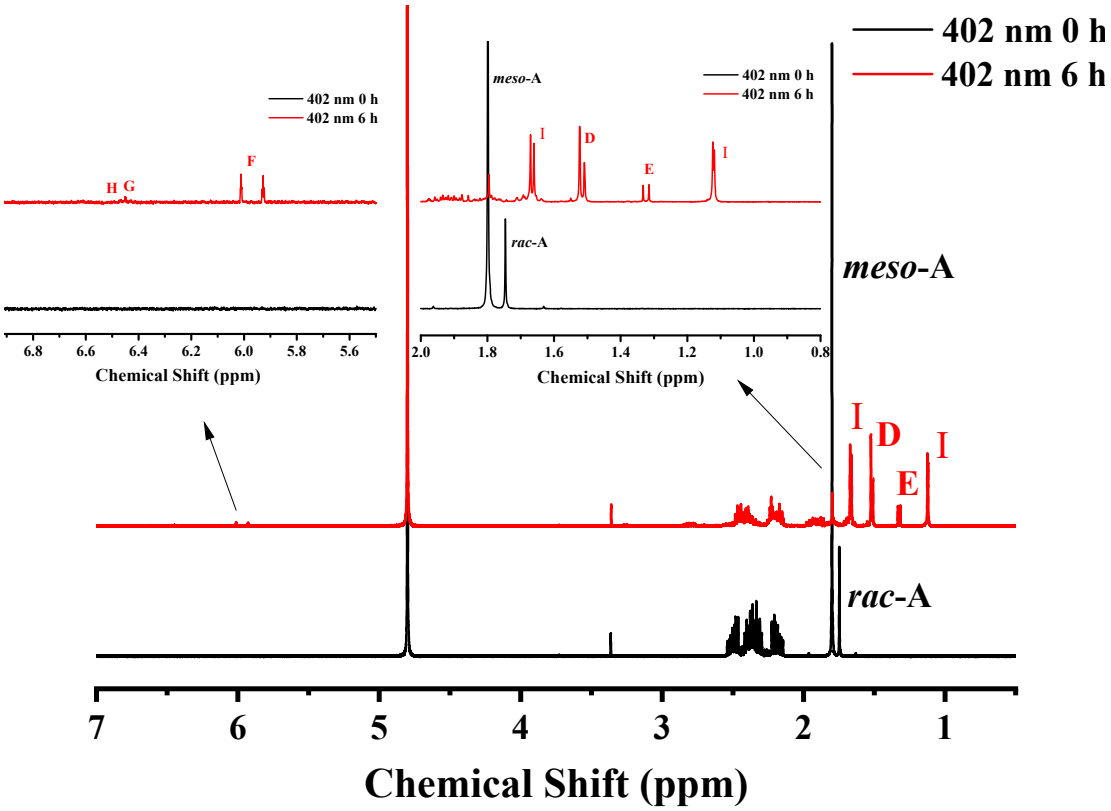

Figure S2. ^{1}H NMR spectra for product mixture before and after 6 h at 25 °C under violet (402 nm) irradiation with 0.05 M solutions of ACPA in 0.1 M Na_2CO_3 in D_2O. Signals used for product determination are assigned to **G** (6.46 ppm), **H** (6.62 ppm), **F** (6.02, 5.94 ppm), *meso*-**A** (1.81 ppm), *rac*-**A** (1.76 ppm), **D** (1.54, 1.52 ppm), **E** (1.34 ppm) and **I** (1.13 ppm).

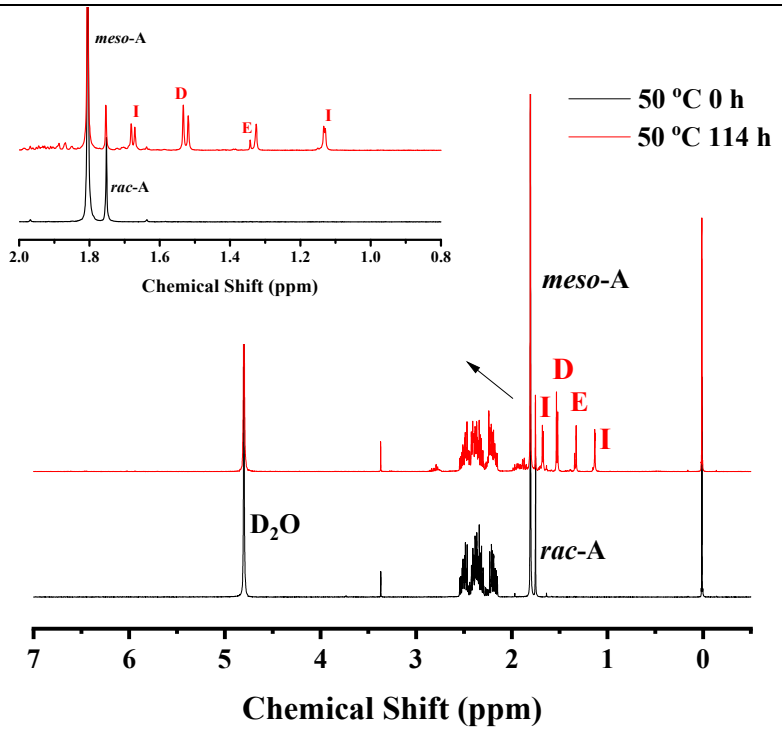

Figure S3. ^{1}H NMR spectra for product mixture before and after 114 h at 50.0 °C with 0.05 M solution of ACPA in 0.1 M Na_2CO_3 in D_2O. Signals used for product determination are assigned to *meso*-**A** (1.81 ppm), *rac*-**A** (1.76ppm), **D** (1.54 ppm, 1.52 ppm), **E** (1.34 ppm), **C** (1.33 ppm, partially overlapped with signal for **E**) and **I** (1.13 ppm).

2D NMR. ^{1}H-^{13}C HSQC (Figure S4), ^{1}H-^{1}H COSY (Figure S5) and ^{1}H-^{13}C HMBC (Figure S6) NMR spectra were obtained to confirm the assignment of signals to the decomposition products formed from ACPA. The HSQC NMR spectrum (Figure S4) clearly shows the signals for the primary, secondary and tertiary carbons. The COSY NMR spectrum (Figure S5) shows cross-peak between protons 16 and 17 consistent with compound **E**. Furthermore, in the HMBC NMR spectrum,there is no cross-peak between proton 9 in the ^{1}H NMR and the nitrile region of the ^{13}C NMR spectrum (cross peaks are present for all nitrile-containing compounds). The cross peaks 9a, 10a, 10b, 10c and 10d in Figure S6 are consistent with compound **I**.

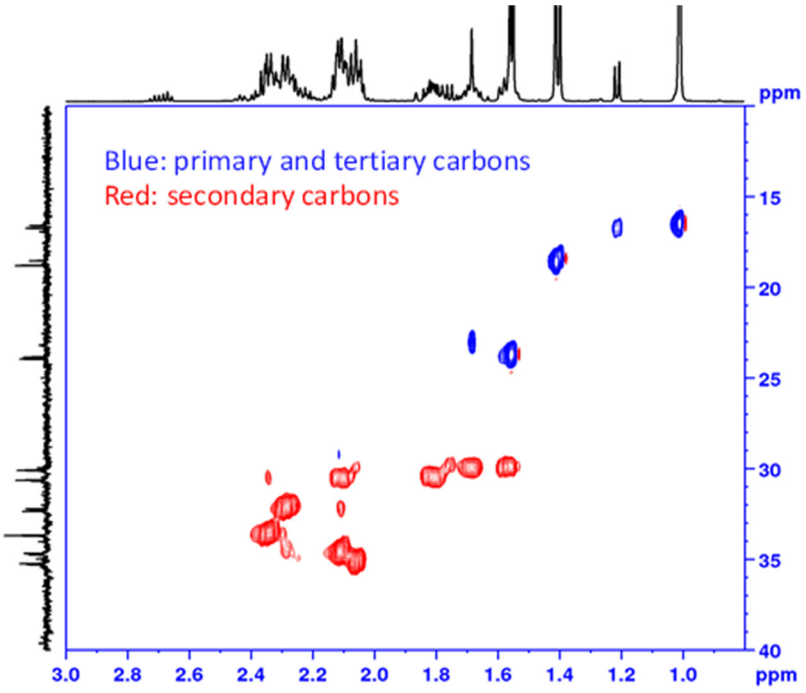

Figure S4. ^{1}H-^{13}C HSQC NMR spectrum of product mixture after 6 h at 25 °C under violet light (402 nm) irradiation with 0.05 M solutions of ACPA in 0.1 M Na_2CO_3 in D_2O.

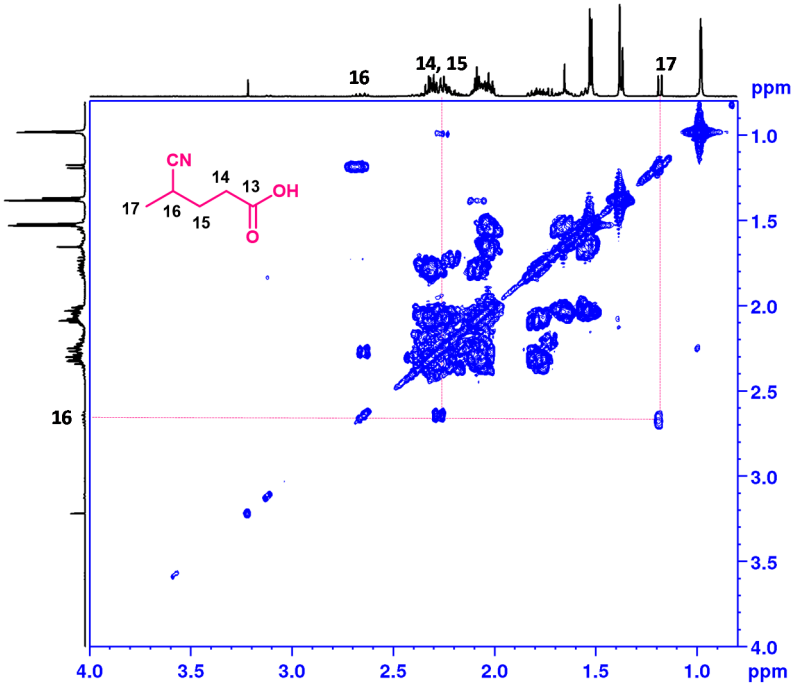

Figure S5. ^{1}H-^{1}H HMBC NMR spectrum of product mixture after 6 h at 25 °C under violet light (402 nm) irradiation with 0.05 M solutions of ACPA in 0.1 M Na_2CO_3 in D_2O.

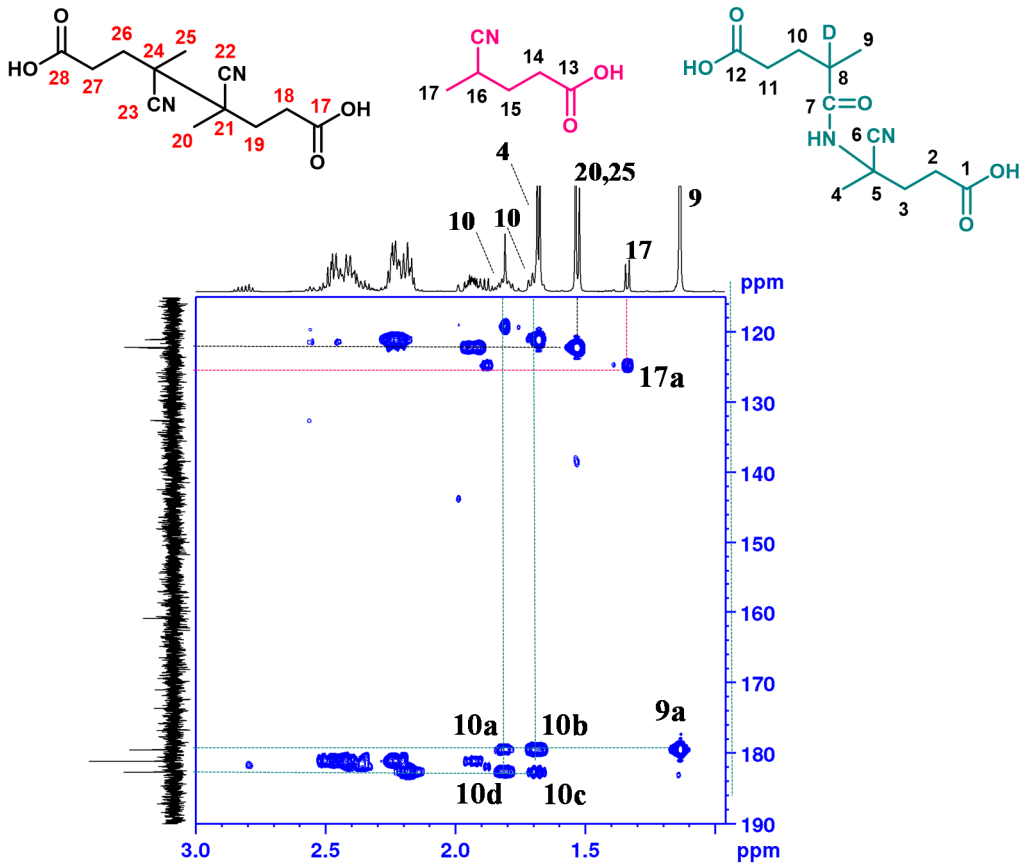

Figure S6. ^{1}H-^{13}C HMBC NMR spectrum of product mixture after 6 h at 25 °C under violet light (402 nm) irradiation with 0.05 M solutions of ACPA in 0.1 M Na_2CO_3 in D_2O. Signals assigned as 20 and 25 are for methyl groups of the two diastereoisomers of D (HMDA and LMDA).

Kinetic Experiments. The decomposition of the two diastereoisomers of 4,4'-azobis (4-cyanopentanoic acid) (ACPA, designated *meso*-A and *rac*-A) and the appearance of products as a function of time for various reaction conditions are shown in Figure S7, Kinetic plots showing rate of disappearance of ACPA from which the rate constants (k_d) were estimated are shown in Figure S16. The extracted rate constants are provided in Table S1 and the Arrhenius parameters estimated on the basis of these data are shown in Table S2.

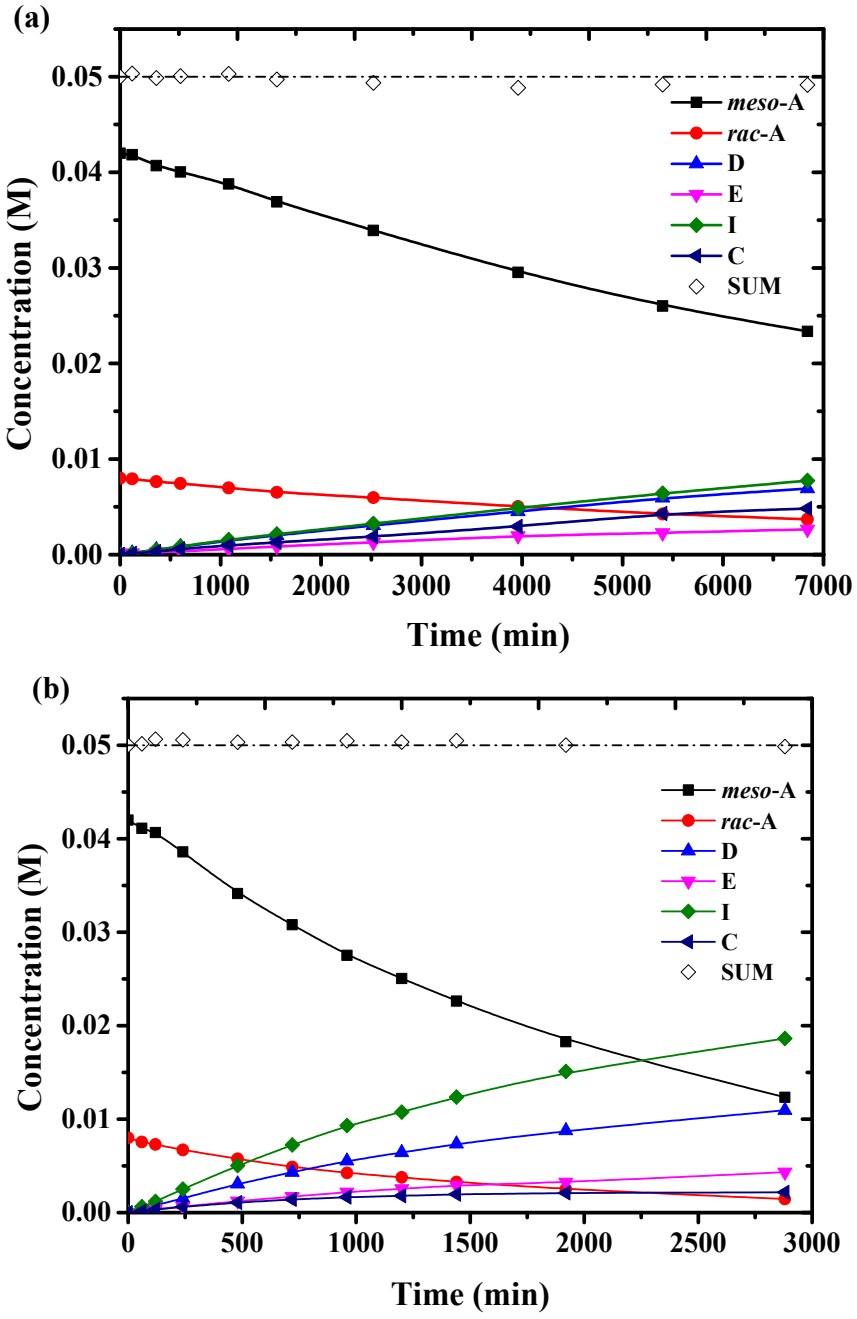
(a)
Concentration (M)
Time (min)
meso-A
rac-A
D
E
I
C
SUM
(b)
Concentration (M)
Time (min)
meso-A
rac-A
D
E
I
C
SUM

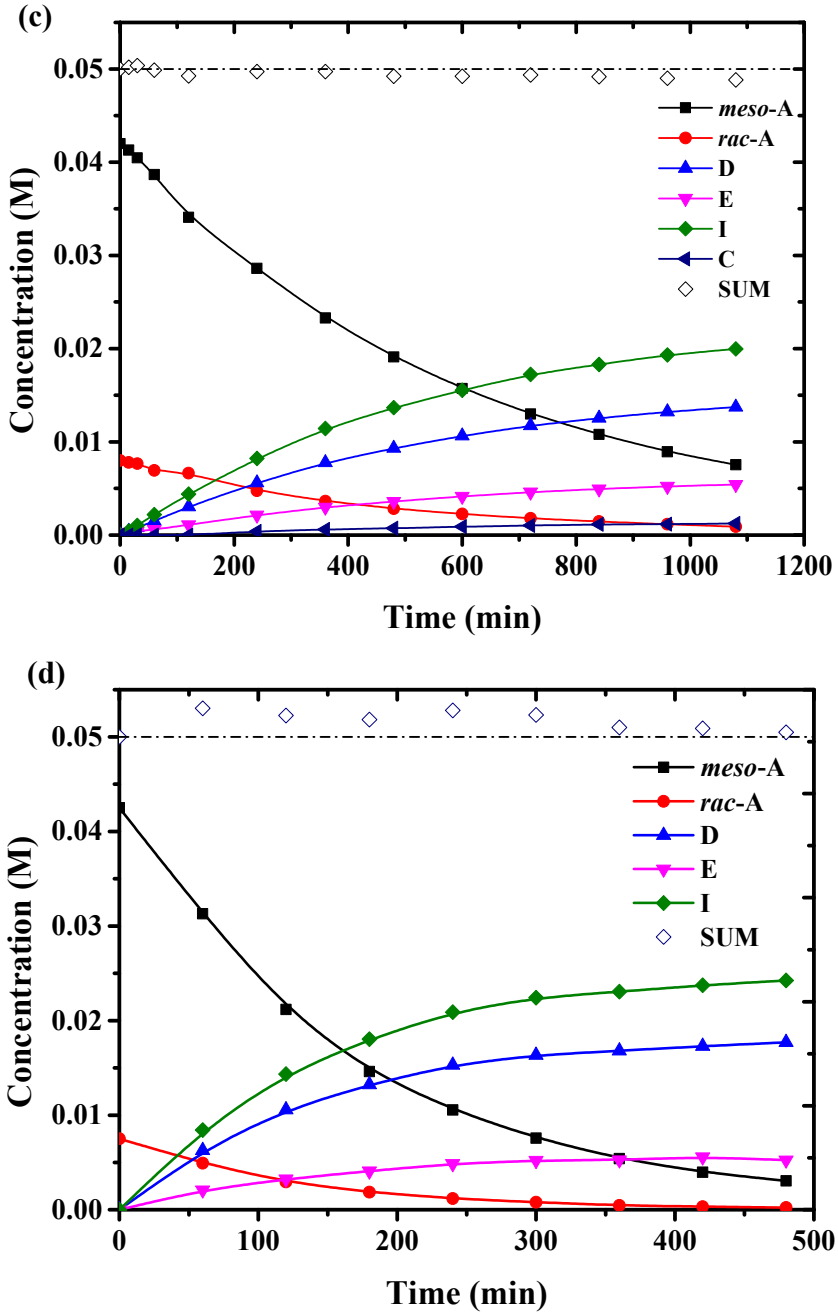

Figure S7. Product-time profiles observed for decomposition of 4,4'-azobis (4-cyanopentanoic acid) (ACPA) at (a) 50.0, (b) 60.0, (c) 70.0 and (d) 80.0 °C with 0.05 M solutions of ACPA with 0.1 M Na_2CO_3 in D_2O, (e) at 25 °C under violet light (402 nm) irradiation with 0.05 M solutions of ACPA in 0.1 M Na_2CO_3 in D_2O.

Reactions in DMF-d_7.

For the decomposition of ACPA under violet light irradication we observe formation of a species, which might be assigned as the isomers of the ketenimine **C**, or a compound derived from it (**I**'). The product is transient and the relevant signals disappear from the NMR spectrum when the solution is allowed to stand at ambient temperature. Isomer 1 has a doublet at ~1.2 ppm, sharp singlet at 1.6 ppm, isomer 2 has a doublet at ~1.2 ppm and a doublet at 1.7 ppm. **I'** may be the iminoester formed by intramolecular reaction of the ketenimine with the carboxy functionality (refer Scheme S1). There is some precedent for this transformation.[3]

The compound **C** or **I'** disappears to form 3 compounds. Two of these are tentatively associated with amide **I** also observed in the D_2O experiments. Consistent with this interpretation, we observed peaks in the LCMS with m/e 269 with similar retention to those seen for ACPA decomposition in D_2O (where m/e 270 was observed due to deuterium incorporation).

Our motivation for this experiment was to see whether on photoirradiation in DMF, we might see a product distribution more similar to that seen by Overberger and Labianca, who observed **G** and **H** as major products. Note that their conditions (UV irradiation, medium pressure mercury lamp, at −40 °C in THF) were significanty different to those used in the present work (violet light irradiation, 402 nm, at 25 °C in DMF).

Where an asterisk appears following a chemical shift in the listing that follows, the NMR signal could not be seen directly due to peak overlap. However, it was possible to ascertain the chemical shift from 2D NMR (HMBC or HSQC) spectra.

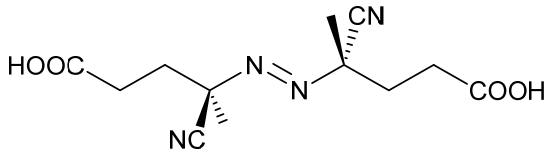

meso-**A**

meso **A**:[2] ^{1}H NMR (DMF-d_7) δ 1.80 (s, 6H, CH_3), 2.32-2.58 (m, CH_2), ^{13}C NMR δ 33.3 (**C**H_2CH_2COOH), 72.4 (**C**(CN)CH_3), 118.5 (CN).

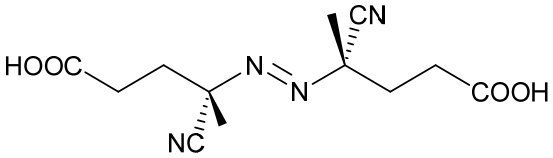

rac-**A**

rac **A**:[2] ^{1}H NMR (DMF-d_7) δ 1.75 (s, 6H, CH_3), 2.32-2.58 (m, CH_2), ^{13}C NMR δ 33.3 (**C**H_2CH_2COOH), 72.3 (**C**(CN)CH_3),118.6 (CN).

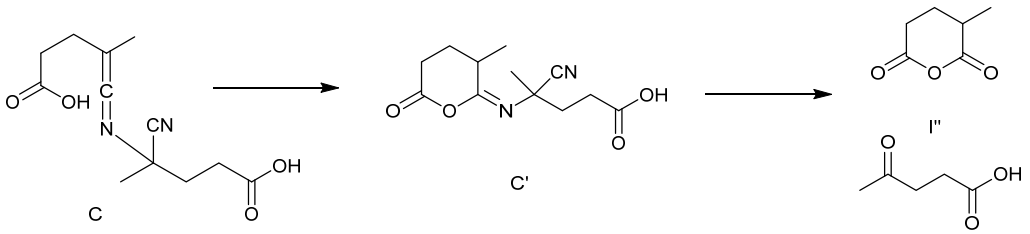

Scheme S1. Proposed pathway for decomposition of the ketenimines **C**.

C' (diastereoisomer 1): ^{1}H NMR (DMF-d_7) δ 1.21 (d, J=6.72 Hz, 3H, C**H**$_3$CH), 1.61 (3H, C(CN)C**H**$_3$), 2.80* (C**H**CH$_3$).

C' (diastereoisomer 2): ^{1}H NMR (DMF-d_7) δ 1.22 (d, J=6.75 Hz, 3H, C**H**$_3$CH), 1.72 and 1.73 (3H, C(CN)C**H**$_3$), 2.80* (C**H**CH$_3$).

I'' : ^{1}H NMR (DMF-d_7) δ 1.25 (d, J = 6.96 Hz, 3H, C**H**$_3$CH(X), 1.79* (C(CX)C**H**H) 1.98* (C(CX)CH**H**), 2.80* (CH$_3$C**H**(X)), ^{13}C NMR δ 24.42 (C(CX)**C**H$_2$), 38.54 (CH$_3$**C**(X)), 173.6 (CH$_2$**C**O), 176.3 (**C**OCH(X)).

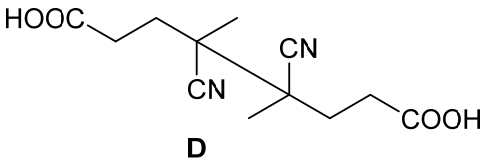

D

2 diastereoisomers

D (LMDA): ^{1}H NMR (DMF-d_7) δ 1.55 (s, 6H, C**H**$_3$), ^{13}C NMR δ 29.80 (C**C**H$_2$), 44.23 (**C**CH$_2$), 121.40 (CN).

D (HMDA): ^{1}H NMR (DMF-d_7) δ 1.56 (s, 6H, C**H**$_3$), ^{13}C NMR δ 29.80 (C**C**H$_2$), 44.23 (**C**CH$_2$), 121.40 (CN).

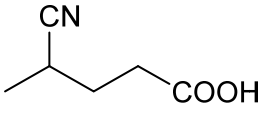

E

E:[2] ^{1}H NMR (DMF-d_7) δ 1.32 (d, J = 7.06 Hz, 3H, C**H**$_3$CH(CN)), 2.02* (m, 2H, CHC**H**$_2$), 2.95 (m, 1 H, CH$_3$C**H**(CN)), ^{13}C NMR δ 17.43 (**C**H$_3$CH(CN)), 24.71 (CH$_3$**C**H(CN)), 29.41 (CH**C**H$_2$), 123.13 (CN), 173.80 (**C**OOH).

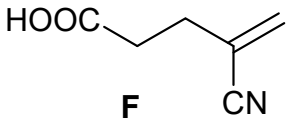

F

F:[2] ^{1}H NMR (DMF-d_7) δ 6.05 (t, *J*=1.1 Hz, 1H, C=C**H**H (*trans* to nitrile)) 6.01 (t, *J*=1.5 Hz, 1H, C=CH**H** (*cis* to nitrile)), 2.59* (2H, C**H**$_2$(CN)C=), 2.52* (C**H**$_2$COOH). ^{13}C NMR δ 29.60 (C=**C**H$_2$), 118.7 (**C**=CH$_2$), 122.0 (**C**N), 131.9 (C=**C**H$_2$), 173.43 (**C**OOH).

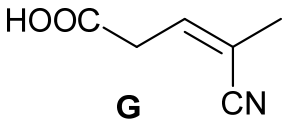

G

G:[2] ^{1}H NMR (DMF-d_7) δ 6.53 (t, *J*=7.71 Hz, 1H, (COOH)CH$_2$C**H**=), δ 3.41* (d, 2H, (COOH)C**H**$_2$CH=), δ 2.03* (s, 3H, =C(CN)C**H**$_3$), ^{13}C NMR δ 19.35 (=C(CN)**C**H$_3$), 111.78 (=**C**(CN)CH$_3$), 141.08 (**C**H=C(CN)CH$_3$), 170.91 (**C**OOH), Signals assigned on basis of 2D NMR.

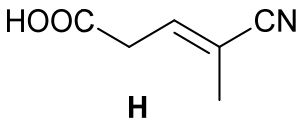

H

H:[2] ^{1}H NMR (DMF-d_7) δ 6.59 (t, *J*=7.43 Hz, 1H, (COOH)CH$_2$C**H**=), δ 3.37* (d, 2H, (COOH)C**H**$_2$CH=), δ 1.94* (s, 3H, =C(CN)C**H**$_3$), ^{13}C NMR 111.8 (=**C**(CN)CH$_3$), 141.1 (**C**H=C(CN)CH$_3$), 170.9 (**C**OOH). Signals assigned on basis of 2D NMR.

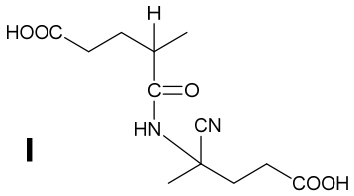

I

2 diastereoisomers

I (diastereoisomer 1): ^{1}H NMR (DMF-d_7) δ 1.09 (d, *J* = 6.86 Hz, 3H, CHC**H**$_3$), 1.66 (3H, C(CN)C**H**$_3$), 2.47* (m, 1H, C**H**CH$_3$), 8.37 (s, 1H N**H**), ^{13}C NMR δ 24.38 (C(CN)**C**H$_3$), 29.40 (**C**H$_2$CH(CH$_3$)), 33.86 (C**C**H$_2$), 39.47 (**C**H(CH$_3$)), 49.68 (**C**(CN)CH$_3$), 120.97 (**C**N), 174.20 (**C**OOH), 175.90 (**C**ONH).

I (diastereoisomer 2): ^{1}H NMR (DMF-d_7) δ 1.10 (d, *J* = 6.87 Hz, 3H, CHC**H**$_3$) 1.67 (3H, C(CN)C**H**$_3$), 2.47* (m, 1H, C**H**CH$_3$), 8.37 (s, 1H N**H**), ^{13}C NMR δ 24.38 (C(CN)**C**H$_3$), 29.40 (**C**H$_2$CH(CH$_3$)), 33.86 (C**C**H$_2$), 39.47 (**C**H(CH$_3$)), 49.68 (**C**(CN)CH$_3$), 120.97 (**C**N), 174.20 (**C**OOH), 175.90 (**C**ONH).

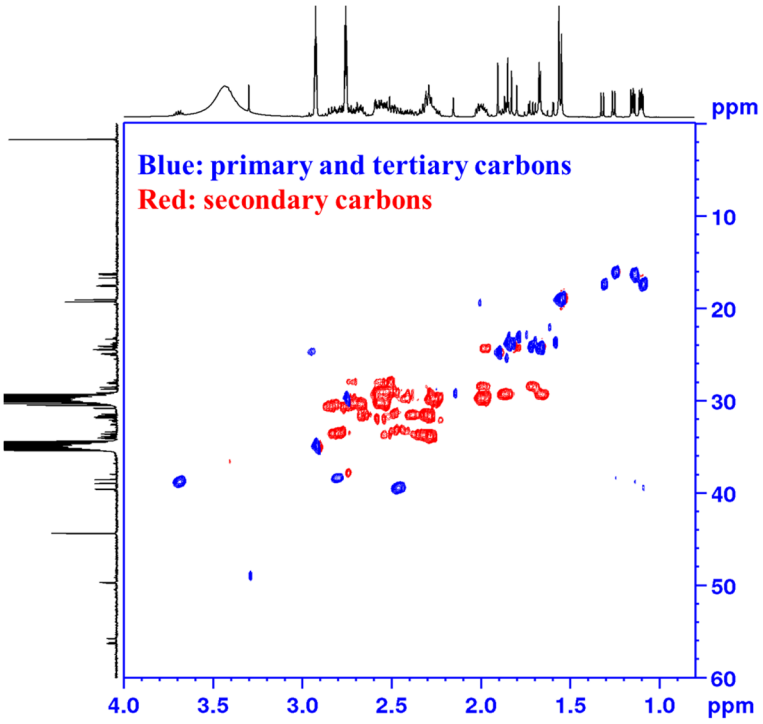

Figure S8. ^{1}H-^{13}C HSQC NMR spectrum of product mixture after 3.5 h at 25 °C under violet light (402 nm) irradiation with 0.05 M solutions of ACPA in 0.1 M Na_2CO_3 in DMF-d_7.

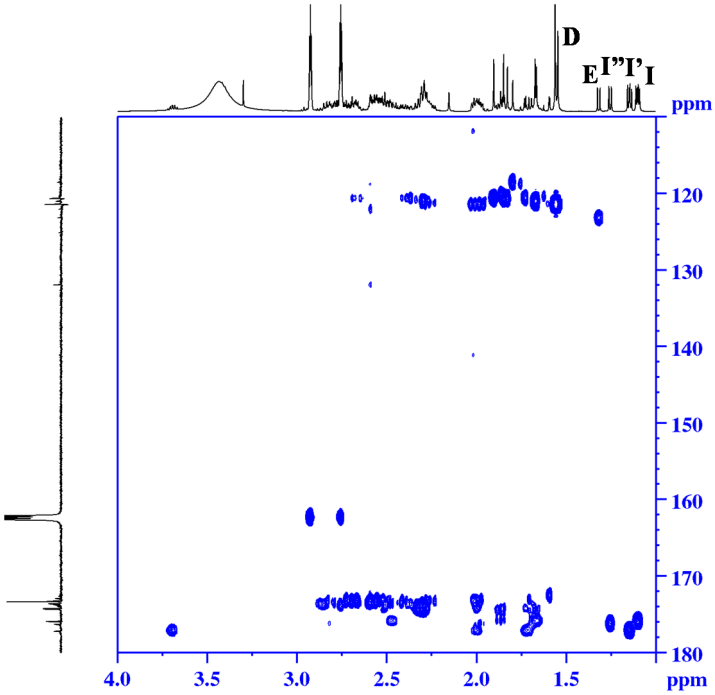

Figure S9. ^{1}H-^{13}C HMBC NMR spectrum of product mixture after 3.5 h at 25 °C under violet light (402 nm) irradiation with 0.05 M solutions of ACPA in 0.1 M Na_2CO_3 in DMF-d_7.

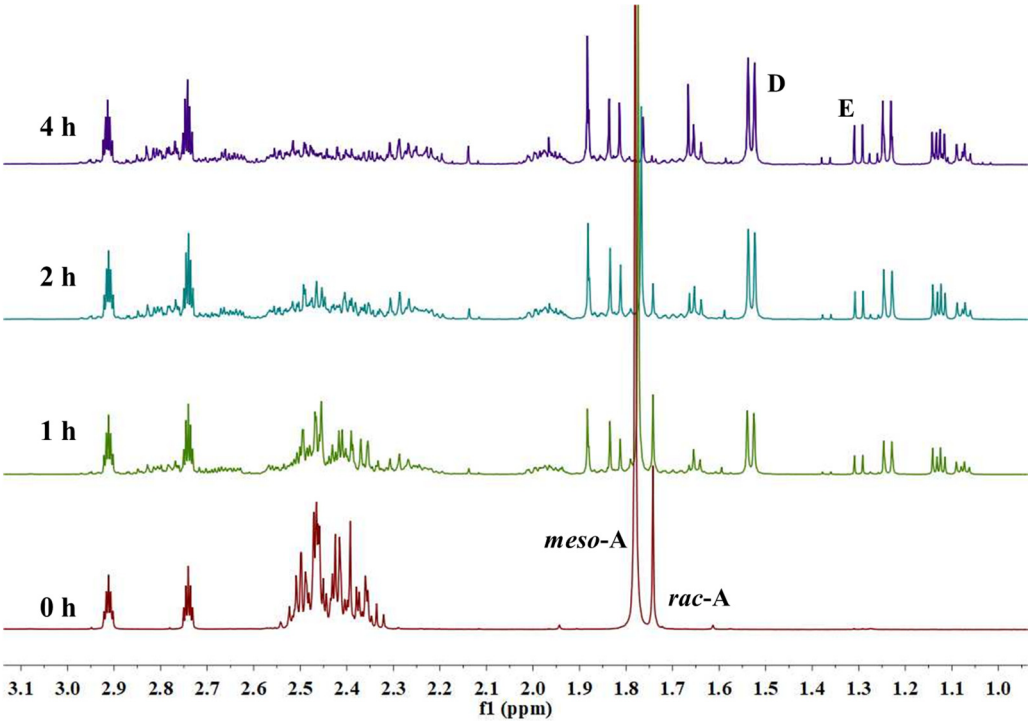

Figure S10. ^{1}H NMR spectra of reaction mixture of decomposition of ACPA after different times at 80 °C in DMF-d_7.

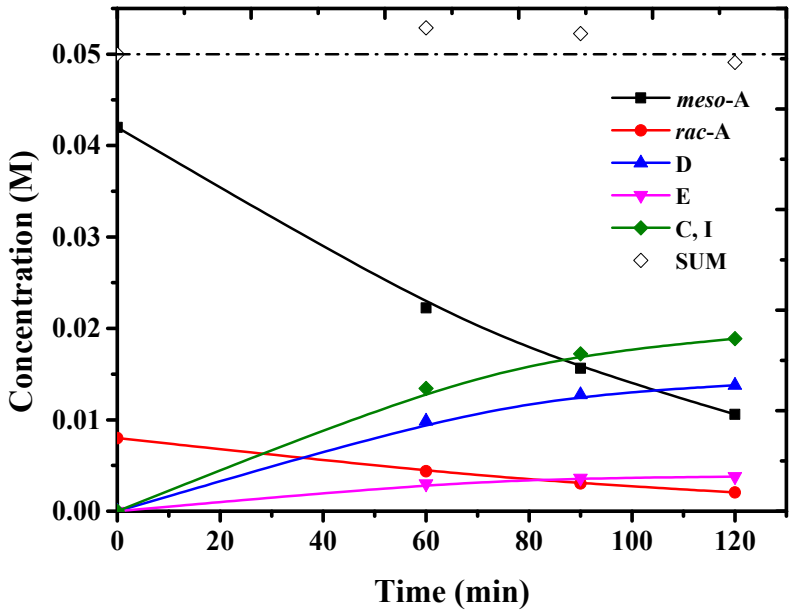

Figure S11. Product-time profiles observed for decomposition of 4,4'-azobis (4-cyanopentanoic acid) (ACPA) at 80.0 °C with a 0.05 M solution of ACPA in DMF-d_7.

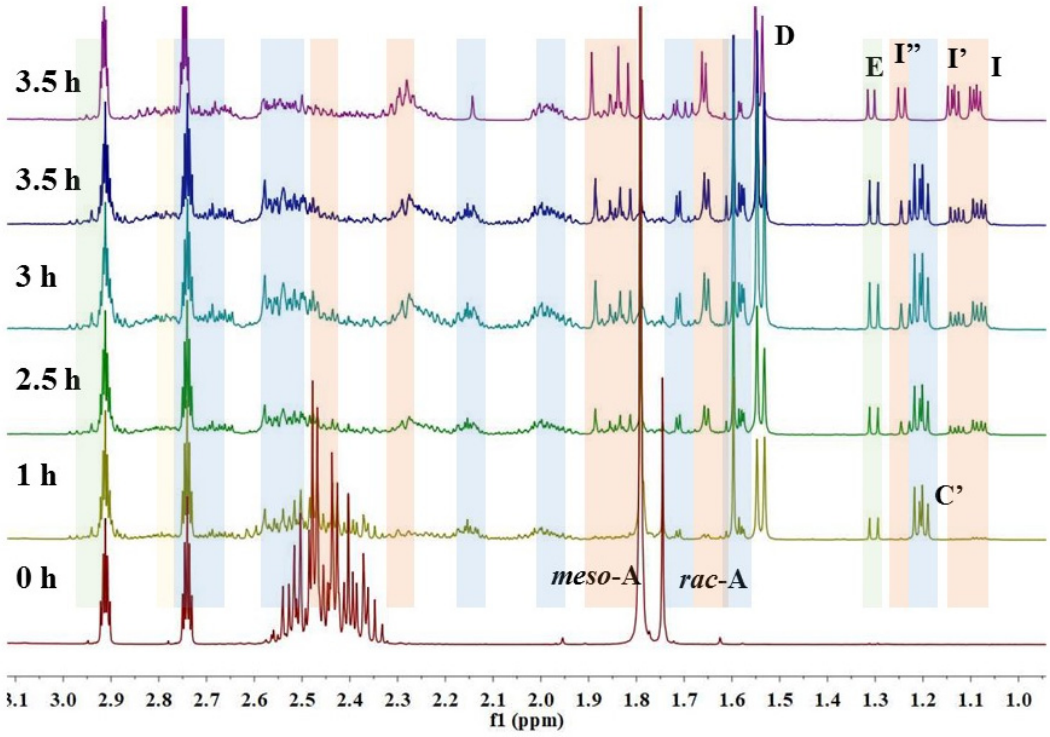

Figure S12. ^{1}H NMR spectra of reaction mixture of decomposition of ACPA as a function of time under 402 nm at 25 °C in DMF-d_7. The uppermost spectrum was obtained after the reaction mixture had been allowed to stand at room temperature for two days. Regions highlighted in blue are for transient species (**C**'). Regions highlighted in orange are for "stable" species (**I**, **I**', **I**").

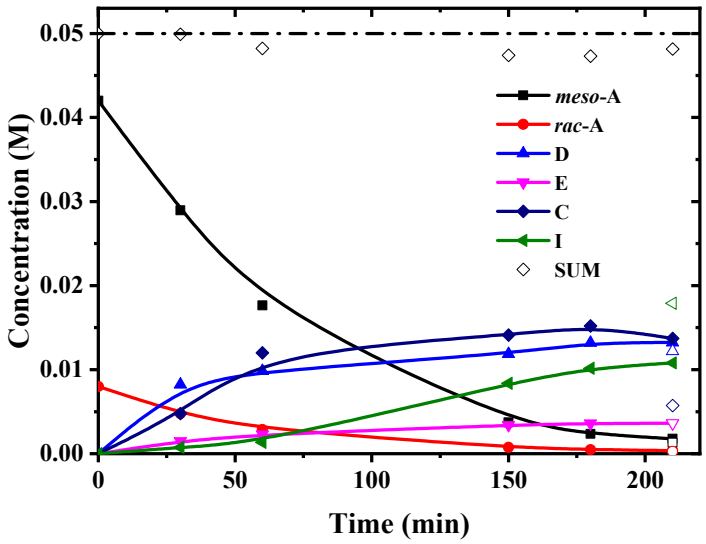

Figure S13. Product-time profiles observed for photo-decomposition of 4,4'-azobis (4-cyanopentanoic acid) (ACPA) at 25.0 °C under violet light irradiation for a 0.05 M solution of ACPA in DMF-d_7. Open symbols (210 min) indicate product distribution for a sample allowed to stand at room temperature for two days. Some scatter may be attributed to the variable length of time between removal of the sample from the photoreactor and obtaining the NMR spectrum.

Products from disproportionation. The products E and F, G and H are formed by disproportionation. In principle, the amount of E formed should equal the amount of F+G+H formed. The product distribution observed for irradiation with 402 nm light at 25.0 °C with a 0.05 M solution of ACPA in DMF-d_7 is consistent with this (Figure S14.

The distribution of the disproportionation products for thermal decomposition of ACPA at 80 °C is shown in Figure S15. Here, the amount of **F** is observed to initially increase then diminish such that the amount of **F**+**G**+**H** << **E**. This is attributed to compound **F** being reactive towards radical addition under the reaction conditions and being converted to oligomers. Note that similar oligomer formation was found during thermal decomposition of AIBN.[4]

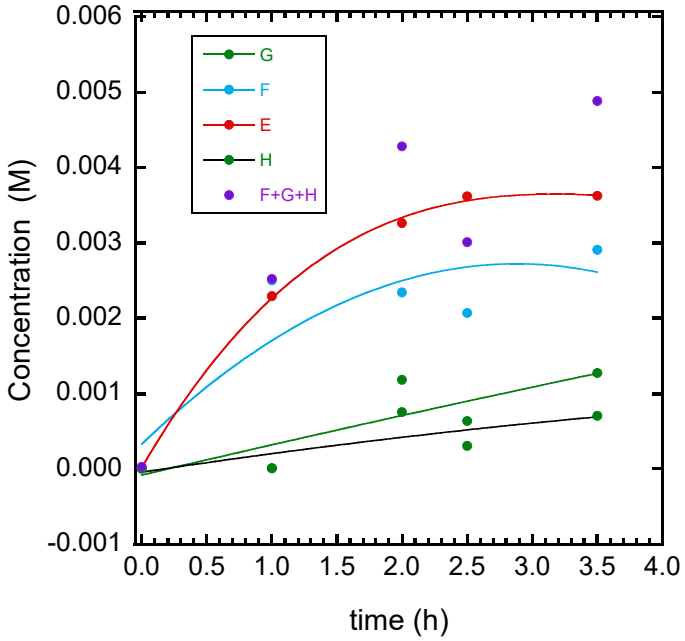

Figure S14. Concentration-time profile for disproportionation products **E**, **F**, **G** and **H** observed during decomposition of 4,4'-azobis (4-cyanopentanoic acid) (ACPA) under irradiation with 402 nm light at 25.0 °C for a 0.05 M solution of ACPA in DMF-d_7.

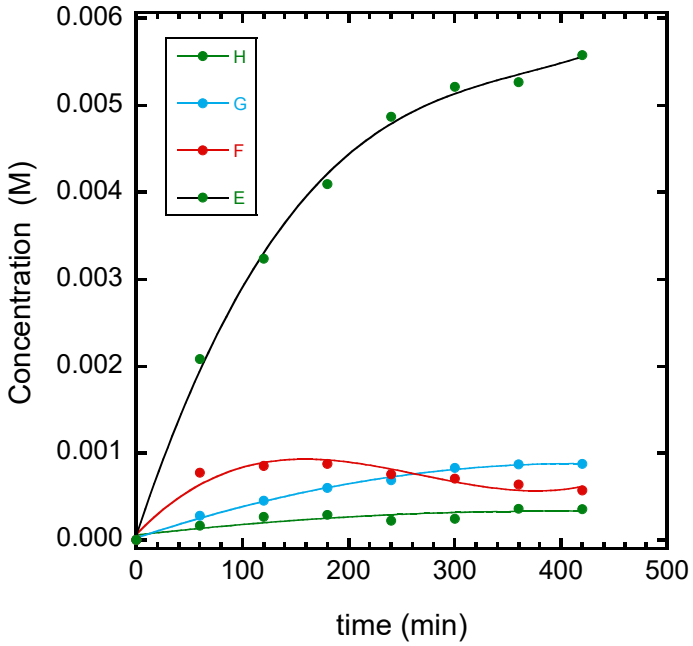

Figure S15. Concentration-time profile for disproportionation products **E**, **F**, **G** and **H** observed during decomposition of 4,4'-azobis (4-cyanopentanoic acid) (ACPA) at 80.0 °C with a 0.05 M solution of ACPA with 0.1 M Na_2CO_3 in D_2O.

Rate coefficients. The rate coefficients (Figure S16, Table S1) are based on the amounts of *meso*-**A** and *rac*-**A** determined by NMR and the data shown in Figure S7. These data were used to determine the Arrhenius parameters (

Table **S2** and Figure 5a).

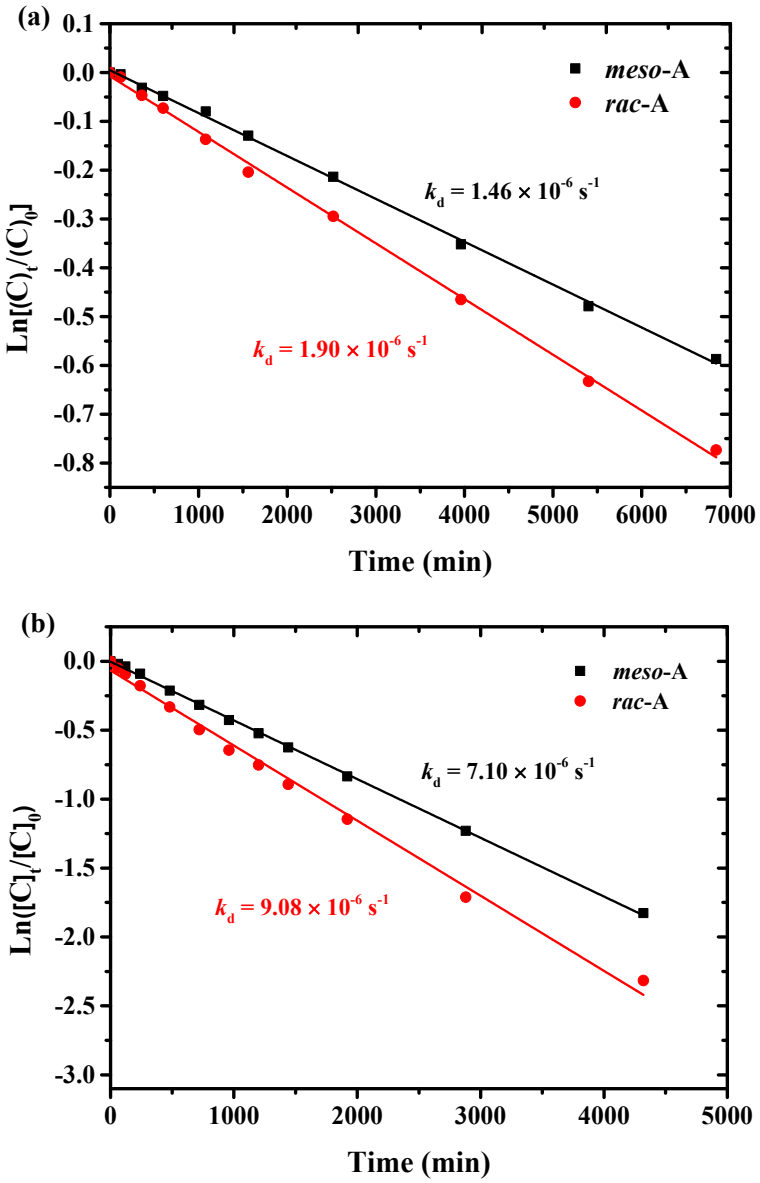

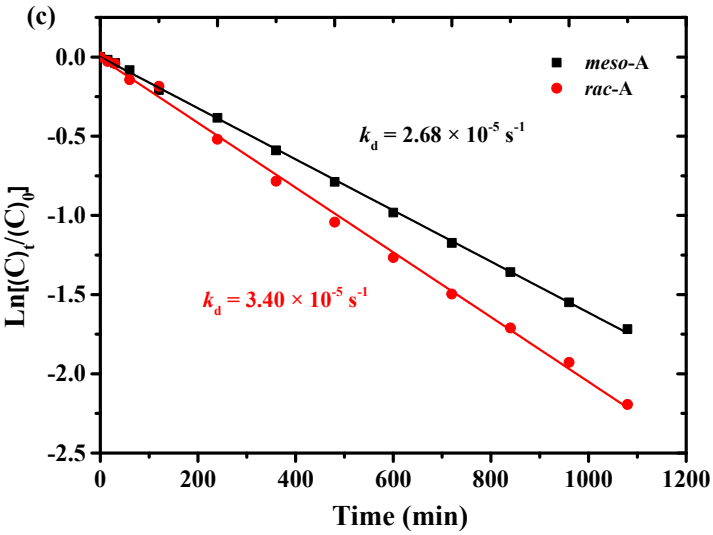
(c)
meso-A
rac-A
$k_d = 2.68 \times 10^{-5}$ s^{-1}
$k_d = 3.40 \times 10^{-5}$ s^{-1}
Ln[(C)$_t$/(C)$_0$]
Time (min)

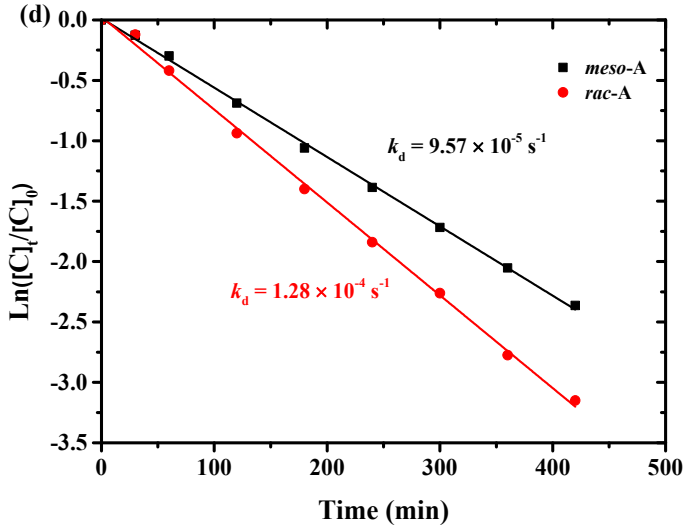
(d)
meso-A
rac-A
$k_d = 9.57 \times 10^{-5}$ s^{-1}
$k_d = 1.28 \times 10^{-4}$ s^{-1}
Ln[C]$_t$/[C]$_0$)
Time (min)

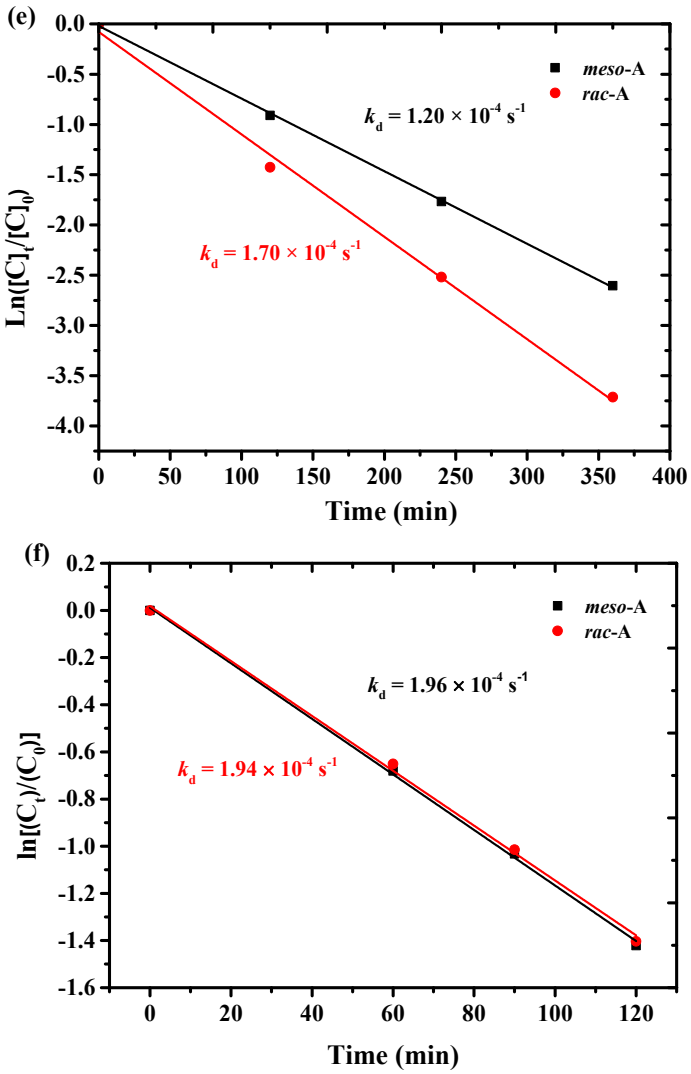

Figure S16. Kinetic plots showing rate of disappearance of the two diastereoisomers of 4,4'-azobis (4-cyanopentanoic acid) (ACPA) at (a) 50.0, (b) 60.0, (c) 70.0 and (d) 80.0 °C, (e) at 25 °C under violet light (402 nm) irradiation with 0.05 M solutions of ACPA in 0.1 M Na_2CO_3 in D_2O, and (f) 80.0 °C with a 0.05 M solution of ACPA in DMF-d_7.

Table S1. Rate coefficients for decomposition of 4,4'-azobis (4-cyanopentanoic acid) (ACPA) based on slopes of lines shown in Figure S16.

		meso-ACPA	*rac*-ACPA	Plot[a]
Temperature (°C)	Na_2CO_3	k_d ($\times 10^{-6}$ s^{-1})	k_d ($\times 10^{-6}$ s^{-1})	
50.0 (D_2O)	0.1	1.46±0.005	1.90±0.008	(a)
60.0 (D_2O)	0.1	7.10±0.014	9.08±0.064	(b)
70.0 (D_2O)	0.1	26.8±0.045	34.0±0.125	(c)
70.0 (D_2O)	0.05	27.7±0.133	35.1±0.142	Not shown
80.0 (D_2O)	0.1	95.7±0.376	128±0.626	(d)
80.0 (DMF-d_7)	0.1	196±2.079	194±2.917	(f)

[a] refer Figure S16

Table S2. Arrhenius parameters for decomposition of 4,4'-azobis (4-cyanopentanoic acid) (ACPA) in aqueous sodium carbonate.

meso-ACPA		*rac*-ACPA	
log(A/s^{-1})	E_a (kJ mol^{-1})	log(A/s^{-1})	E_a (kJ mol^{-1})
15.47±0.19	131.65±0.98	15.69±0.15	132.24±1.26

Product distribution

The ratio of C:C combination:C-N combination:disproportionation was evaluated from the integrals of signals assigned to (**D**+**D'**) : (**I**+**C**) : **E**, respectively. If the formation of ketenimine is irreversible this ratio should be constant for a given set of conditions and this appears to be the case except for very short times, which is attributed to experimental error (Figure S17). The ratio of the unsaturated disproportionation products **F** : **G** : **H** should also be constant and their sum equal to the saturated disproportionation product **E**. However **F** is expected to be reactive towards radicals formed during the reaction. The ratio is therefore estimated as [**E** –(**G**+**H**)] : **G** : **H**. The amounts of **G** and **H** are very small and not reliably estimated in all experiments. The fraction of C-C combination is higher for higher reaction temperatures (Figure S18).

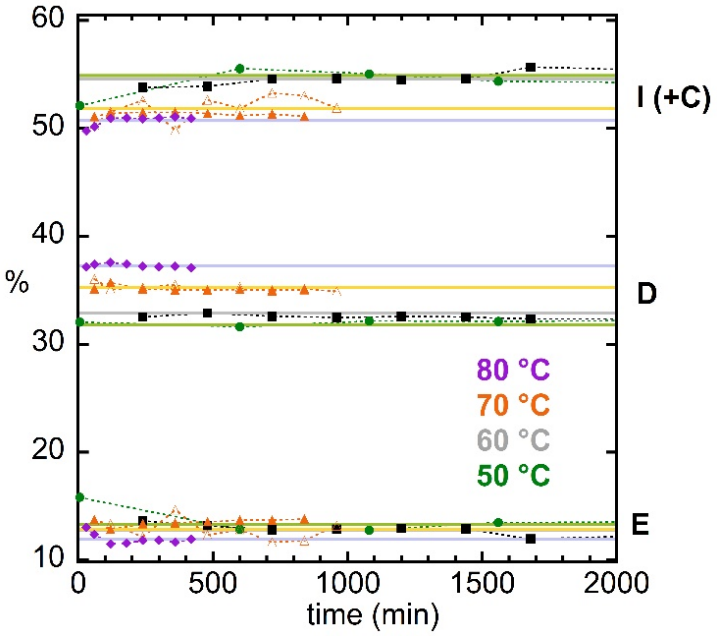

Figure S17. Percent of C:C combination:C-N combination:disproportionation [(**D**+**D**') : (**I**+**C**) : **E**] *vs* reaction time in thermal decomposition of ACPA for various temperatures. Data to 2000 min shown.

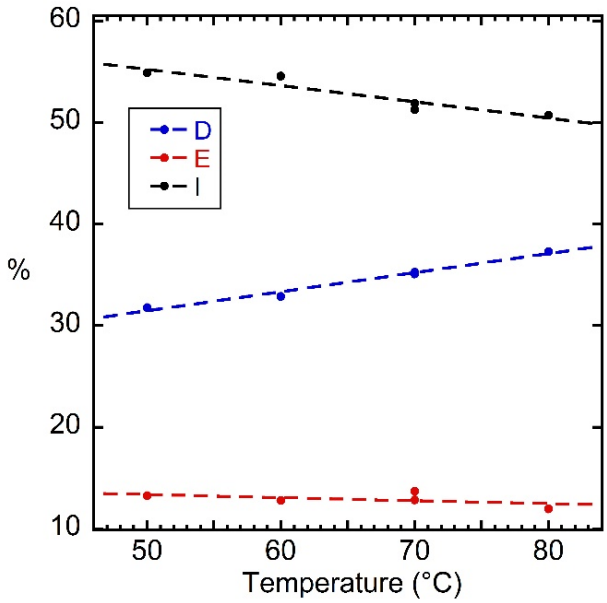

Figure S18. Temperature dependence of C:C combination:C-N combination:disproportionation [(**D**+**D**') : (**I**+**C**) : **E**] in thermal decomposition of ACPA. Based on average values shown in Figure S17.

References

1. Aerts, A.; Lewis, R. W.; Zhou, Y.; Malic, N.; Moad, G.; Postma, A., Light-Induced RAFT Single Unit Monomer Insertion in Aqueous Solution– Towards Sequence-Controlled Polymers. *Macromol. Rapid. Commun.* **2018,** *39* (19), 201800240.
2. Overberger, C. G.; Labianca, D. A., Azo compounds. Investigation of optically active azonitriles. *J. Org. Chem.* **1970,** *35*, 1762-1770.
3. Lu, P.; Wang, Y., The thriving chemistry of ketenimines. *Chem. Soc. Rev.* **2012,** *41* (17), 5687-5705.
4. Krstina, J.; Moad, G.; Willing, R. I.; Danek, S. K.; Kelly, D. P.; Jones, S. L.; Solomon, D. H., Further studies on the thermal decomposition of AIBN - Implications as to the mechanism of termination in methacrylonitrile polymerization. *Eur. Polym. J.* **1993,** *29* (2/3), 379-88.